Published in final edited form as:
Mol Cancer Ther. 2009 May ; 8(5): 1106–1112. doi:10.1158/1535-7163.MCT-08-0779.

Antibodies targeting hepatoma-derived growth factor as a novel strategy in treating lung cancer

Hening Ren[1], **Zuoming Chu**[1], and **Li Mao**[1,2]

[1] Department of Thoracic/Head and Neck Medical Oncology, The University of Texas M. D. Anderson Cancer Center, Houston, Texas

[2] Cancer Biology Program, The University of Texas Graduate School of Biomedical Sciences at Houston, Houston, Texas

Abstract

Hepatoma-derived growth factor (HDGF) is overexpressed in lung cancer and the overexpression correlates with aggressive biologic behaviors and poor clinical outcomes. We developed anti-HDGF monoclonal antibodies and tested their anti-tumor activity in lung cancer xenograft models. We also determined biologic effects in tumors treated with the antibody alone or in combination with bevacizumab/avastin (an anti-VEGF antibody) and/or gemcitabine (a chemotherapeutic agent). We found the anti-HDGF was effective to inhibit tumor growth in non-small cell lung cancer (NSCLC) xenograft models. In the A549 model, comparing to control IgG, tumor growth was substantially inhibited in animals treated with anti-HDGF antibodies, particularly HDGF-C1 ($P = 0.002$) and HDGF-H3 ($P = 0.005$). When HDGF-H3 was combined with either bevacizumab or gemcitabine, we observed enhanced tumor growth inhibition, particularly when the three agents were used together. HDGF-H3-treated tumors exhibited significant reduction of microvessel density with a pattern distinctive from the microvessel reduction pattern observed in bevacizumab-treated tumors. HDGF-H3 but not bevacizumab treated tumors also showed a significant increase of apoptosis. Interestingly, many of the apoptotic cells in HDGF-H3-treated tumors are stroma cells, suggesting the mechanism of the anti-tumor activity is, at least in part, through disrupting formation of tumor-stroma structures. Our results demonstrate that HDGF is a novel therapeutic target for lung cancer and can be effectively targeted by an antibody-based approach.

Keywords

HDGF; NSCLC; antibody; therapy

INTRODUCTION

Lung cancer is the leading cause of cancer-related deaths worldwide (1). Most of the patients with lung cancer are diagnosed at advanced stage with a median survival <12 months due to lack of effective therapies (2–4). Therefore, development of novel therapeutics for patients with advanced stage of lung cancer is critically needed.

Hepatoma-derived growth factor (HDGF) is a heparin-binding growth factor identified from media conditioned by a human hepatoma-derived cell line, and exhibits mitogenic activity to

Request for reprints: Li Mao, M.D., Department of Thoracic/Head and Neck Medical Oncology, Unit 432, The University of Texas M. D. Anderson Cancer Center, 1515 Holcombe Boulevard, Houston, TX 77030. Phone: (713) 792-6363; Fax: (713) 796-8655; E-mail: lmao@mdanderson.org.

various cell types (5–7). HDGF is highly expressed during embryonic development in smooth muscle, guts, and endothelium but not after birth (5,8,9). It has also been implicated in angiogenesis (8). High-level HDGF can be observed in various human cancers including lung cancer and the overexpression is correlated with poor clinical outcomes (10–14), suggesting the importance of HDGF in cancer progression. Although the molecular mechanisms of HDGF in cancer progression are poorly understood, we have previously showed that HDGF contributes to anchorage independent growth and tumor cell invasion (15). We further demonstrated that lung cancer cells with down-regulated HDGF formed significantly smaller tumors *in vivo* (15), suggesting HDGF may be a therapeutic target.

In this study, we reported an antibody based approach to target HDGF in non-small cell lung cancer (NSCLC) models.

MATERIALS AND METHODS

Cell lines and culture conditions

Human NSCLC cell lines were grown in monolayer culture in a 1:1 mixture of DMEM and Ham's F12 medium supplemented with heat inactivated 5% fetal bovine serum and antibiotics at 37°C in a humidified atmosphere consisting of 95% air and 5% CO_2 unless indicated otherwise.

Recombinant protein

The cDNA fragment that encodes HDGF was PCR amplified and cloned into pGEX-4-T1 vector (GE Health Care, Piscataway, NJ). The resulted plasmid, pGST-HDGF, was used to generate GST-HDGF fusion protein in E. Coli strain BL21 (DE3). The recombinant protein was purified using GST affinity chromatography.

Hybridoma and antibody production

Balb/c mice were immunized with the fusion protein and boosted twice. Three days after the last boost, mice were sacrificed and spleenocytes were fused with P3X63Ag8.653 cells followed by culturing in selecting medium. Anti-HDGF antibody secreting hybridoma clones were identified and verified. For large scale antibody production, hybridoma cells were cultured in RPMI 1640 supplemented with Nutridoma CS (Roche Applied Science, Indianapolis, IN). The antibodies were purified using protein G-agarose (GE Health Care) affinity chromatograph. Purified antibody was then dialyzed and sterile filtered through a 0.22μm filter.

Protein extraction and Western blotting

Log-phase growing NSCLC cells were incubated in PBS with 1% Triton X-100 and protease inhibitor cocktail (Roche Applied Science). The cell lysates were clarified by centrifugation. Proteins (10μg) were separated through a 10% polyacrylamide gel and transferred to a nitrocellulose membrane (Schleicher & Shuell BioScience, Keene, NH). Signal was detected using an enhanced chemiluminescence kit (Pierce, Rockford, IL).

Immunoprecipitation

Protein extracts were incubated with anti-HDGF antibody immobilized on protein G-agarose (Sigma, St. Luis, MO) for 2 hrs. Bound proteins were eluted with 2 X SDS-PAGE sample loading buffer. The eluted proteins were analyzed using SDS-PAGE and Western blotting.

Immunohistochemistry

Sections (4 μm) were from formalin-fixed and paraffin-embedded tissue blocks or OCT-embedded frozen tissues. All the sections were mounted on positively charged glass slides. For formalin-fixed tissues, sections were deparafinized and stained with appropriate antibody using ABC Elite system (Vector Labs, Burlingame, CA). For frozen tissues, the sections were fixed with acetone before being processed for staining. Diaminobenzidine was used as a chromogen and commercial hematoxylin was used for counterstaining. For microvessel density analysis, CD31 staining was measured using 10X objective magnification for 3 to 6 randomly selected fields (2.18 mm^2 per field). Each field was then divided into 155 squares (grids). The grids with CD31 staining was counted as positive and total positive grids divided by the total grids measured was used to calculate percentage of positive grids for each sample.

TUNEL assay

Tissue sections were incubated with TdT reaction buffer containing 0.2 unit/μl terminal transferase (New England Biolabs, Ipswich, MA) and 20 μM biotin-16-dUTP (Roche Applied Science) in a humidify chamber. ABC complex (Vector Labs) was used for signal development. TUNEL positive cells were counted under a 10 X objective lens. Average of number of positive TUNEL cells in 3–5 fields was used as TUNEL labeling index.

Tumor xenograft model

Athymic Swiss nu/nu/Ncr nude (nu/nu) mice were used. Briefly, 4-week-old male nude mice were injected subcutaneously with 4×10^6 cancer cells at a single dorsal site. At day 7, tumor bearing mice were randomized into experimental groups (5 per group) and treated with appropriate agents accordingly. Treatment was repeated every 3 days. Tumor size was measured every 2 days until animals were sacrificed by measuring the tumors in three dimensions with calipers. At the time of sacrifice, tumors were dissected and weighted.

Statistical analyses

Student T-test was used to determine differences in tumor weight, microvessel density, Ki67 labeling index, and TUNEL labeling index, between tumors treated with control antibody (M31) and tumors treated with anti-HDGF antibodies or combinations. Student T-test was also used to determine difference in microvessel density between H3 treated tumors and combinations. P values smaller than 0.05 are considered statistically significant. For *in vivo* tumor growth, the statistical significance of differences in tumor growth was analyzed by ANOVA using analytical software, STATISTICA (StatSoft, Tulsa, OK).

RESULTS AND DISCUSSION

To explore antibody-based therapeutic strategy, we first generated a panel of anti-HDGF antibodies (HDGF-C1, -C4, -H3, and -L5–9) capable to bind native HDGF. All the antibodies are IgG1 and recognize the “classic” HDGF at approximately 38 kDa on Western blots (Fig. 1A) and the identity of the recognized protein was confirmed by immunoprecipitation and subsequent two-dimensional gel electrophoresis based Western blot analysis (Fig. S1). Some of the antibodies can also recognize proteins migrated at 50 to 70 kDa range (Fig. 1A), possibly modified forms of HDGF or HDGF homologues as these proteins can also be recognized by immunoprecipitation and anti-HDGF antibodies different from the antibody used for immunoprecipitation (Fig. S1).

To validate that HDGF is secreted or released from lung cancers, we analyzed proteins from conditioned media of a panel of non-small cell lung cancer (NSCLC), the most common type of lung cancer, cell lines. HDGF was detected in the conditioned media of every

NSCLC cell lines (Fig. 1B). Beside the common 38 kDa band, proteins between 38 kDa and 60 kDa were also observed in some of the cell lines (Fig. 1B). The result indicates that most of the NSCLC cells secret or release substantial amount of HDGF into extracellular space. Because HDGF can reenter into cells (5) or bind to cell surface receptor (16) to assert its mitogenic property, neutralizing the extracellular HDGF is a logical strategy to target HDGF.

To determine distribution of the antibody administered IP, we injected 250μg HDGF-H3 and M31 antibodies labeled with either Cy3 or Cy5 fluorescence dyes to each mouse bearing A549 tumors. We first examined the antibody distribution using a whole body imaging scanner with different filters and found the antibodies were delivered to the entire animal including the tumors (Fig. 1C). We then examined tumor tissues obtained from the mice after treatment using a specific anti-mouse IgG1 antibody. While tumors from PBS treated mice did not show staining as expected, staining was observed in tumors treated with various antibodies (Fig. 1D), indicating the antibodies were delivered to the tumor tissues. Interestingly, we observed cytoplasmic staining in both HDGF-C1 and HDGF-H3 treated tumors, suggesting the antibodies somehow entered into the cells. It was noticed that the cytoplasmic staining was particularly strong in HDGF-C1 treated cells and the staining might concentrate in perinuclear and even inside nuclear in some cancer cells (Fig. S2). The significance of the observation is unclear at this time.

To test the anti-HDGF antibodies in suppressing growth of NSCLC, we evaluated four antibodies in A549 NSCLC xenograft model. Once tumors formed subcutaneously in nude mice, we treated the animals with the anti-HDGF antibodies (10mg/kg, every three days) by intra-peritoneal (IP) injection. Mice treated with the anti-HDGF antibodies showed significantly slower tumor growth compared to mice treated with controls (Fig. 2A). Comparing to MOPC-31 (M31), an IgG1 antibody with no know target, tumor growth was substantially inhibited in animals treated with HDGF-C1 ($P = 0.002$), HDGF-C4 ($P = 0.026$), HDGF-H3 ($P = 0.005$), and HDGF-L5–9 ($P = 0.05$). The average tumor burdens at the end of the experiment (22 days after tumor inoculation) were 960 mg for control-IgG treated mice, compared to 224 mg for HDGF-C1 and 266 mg for HDGF-H3 treated mice, respectively. Consistent with the tumor growth inhibition, the size and weight of the tumors were substantially smaller/lighter in the animals treated with the anti-HDGF antibodies (Fig. 2B and 2C). Because of the superior tumor growth inhibition observed in HDGF-C1 and HDGF-H3 treated animals, the two antibodies were selected for further experimentations. In the subsequent experiments using H460 NSCLC xenograft model and M109 murine lung adenocarcinoma model, both HDGF-C1 and HDGF-H3 showed tumor growth inhibition (data not shown). HDGF-H3 was then selected as the lead antibody for experiments described below.

We did not observe apparent toxicities including weight loss to the animals during 2 weeks treatment. At the time of sacrificing animals, we examined gross appearance of major organs and found no abnormal changes in the antibody treated animals both grossly and histologically (Fig. S3).

Because HDGF has been suggested to promote angiogenesis independent of VEGF (17,18) and the cellular HDGF may be released upon damage by cytotoxic agents, we hypothesized that combining HDGF-H3 antibody with bevacizumab (avastin), a clinically effective VEGF neutralizing antibody, and/or Gemcitabine (Gem), a chemotherapeutic agent approved for NSCLC, may have synergy in treating NSCLC. We test the hypothesis using A549 NSCLC xenogrraft model. Comparing to M31 control, both HDGF-H3 and bevacizumab significantly inhibited tumor growth (Fig. 2D, $P = 0.0002$ and $P < 0.0001$, respectively) whereas Gem showed only a modest tumor growth inhibition ($P = 0.23$). When Gem was

co-administered with HDGF-H3, however, tumors grown slower than those treated with Gem alone. The average final tumor burden was 279mg in the Gem and HDGF-H3 treated animals compared to 500mg in the Gem alone animals, although the difference did not reach statistical significance ($P = 0.13$). However, the inhibition by the two agent combination was only slightly greater compared to HDGF-H3 treatment alone (375 mg average tumor burden), suggesting the effect is mainly due to HDGF-H3. When Gem, HDGF-H3, and bevacizumab were administered together, we observed statistically significant tumor growth inhibition compared to any of the two-agent combinations (P values were 0.002, 0.002, and < 0.0001 comparing to HDGF-H3 + bevacizumab, HDGF-H3 + Gem, and bevacizumab + Gem, respectively). Tumors in 3 of the 7 animals treated with the three-agent combination weighted less than 10 mg at the time the animals were sacrificed. These data demonstrate a potential therapeutic utility of anti-HDGF strategy in treating lung cancer. The data also suggest that the therapeutic strategy may be enhanced by combining with chemotherapy and other targeted agents with distinct biological activities.

To elucidate potential mechanisms of the anti-tumor activity, we examined the tumors obtained at the end of treatments for proliferation using Ki-67, microvessel density using CD31, and apoptosis using TUNEL assay. We found that Ki-67 labeling index was reduced in HDGF-H3 treated tumors (Fig. 3A and 3B), but not in bevacizumab or Gem treated tumors. No significant reduction of Ki-67 labeling indices was observed in tumors treated with combinations. This result suggests that the anti-tumor activity by bevacizumab and Gem was not due to inhibition of cell proliferation. Alternatively, the proliferation capability of the cells regained after prolonged treatment period as the tumors analyzed had been treated for more than 2 weeks.

The microvessel density was substantially reduced in both HDGF-H3 treated ($P < 0.001$) and bevacizumab treated ($P < 0.001$) tumors compared to M31 control antibody treated tumors (Fig. 3C). However, the patterns of microvessel inhibition were distinctive between HDGF-H3 and bevacizumab treated tumors. HDGF-H3 treatment appears to mainly reduce the size or thickness of the vessels (Fig. 3D-*c*) whereas bevacizumab treatment substantially reduced the vessel numbers but not the size (Fig. 3D-*b*), suggesting that HDGF-H3's anti-angiogenic activity might be independent of VEGF. It should be noted that the vessel size observation is not quantitative and needs verification in experiments using quantitative methods. It is well known that bevacizumab can cause fatal pulmonary hemorrhage (19,20), which prevents its use in patients with centrally located lung cancers. Although the mechanism of the side effect has not been fully elucidated, it is possible that the combining the anti-HDGF antibody with bevacizumab may not only enhance their anti-angiogenic activities but also reduce the risk of hemorrhage because the anti-HDGF agent can reduce the vessel size and potentially prevent fatal bleeding. Surprisingly, Gem treatment increased size of microvessels (Fig. 3D-*d*) and the increase was only modestly inhibited by combined treatment with bevacizumab ($P = 0.21$, Fig. 3C–e) but more significantly by combined treatment with HDGF-H3 ($P = 0.04$, Fig. 3C–f). Again, the inhibition was mainly through reduction of the vessel numbers in bevacizumab treated tumors (Fig. 3D–*e*) but reduction of the vessel sizes in HDGF-H3 treated tumors (Fig. 3D–*f*). The notion that bevacizumab and HDGF-H3 inhibit angiogenesis through independent mechanisms is further supported by an enhanced inhibition of microvessel density when the two agents were combined (Fig. 3D–*g* and *h*).

An increased apoptosis was observed in Gem treated tumors, as expected, (Fig. 4A and 4B–*d*) and HDGF-H3 treated tumors (Fig. 4A and 4B–*c*) but not bevacizumab treated tumors (Fig. 4A and 4B-*b*). This result is particularly interesting because the antibody does not trigger apoptosis nor significant growth inhibition of the cancer cells *in vitro* (data not shown), suggesting a role of tumor microenvironment in HDGF-based therapeutic strategy.

In fact, we have observed a substantial increase of apoptotic cells in tumor stroma of HDGF-H3 treated tumors (Fig. 4C) but not in stroma of normal tissues (data not shown). Together with the observation of HDGF-H3 induced microvessel size reduction, the data suggest a possibility that the antibody affects paracytes surrounding the microvessels and causes collapse of the vessels, which is consistent with the paracrine role of HDGF in smooth muscle cells and fibroblasts (5). Combining HDGF-H3 with bevacizumab or Gem increased apoptosis compared to the single agent alone ($P = 0.004$ and $P < 0.001$, respectively; Fig. 4A and B). These results support a utility of anti-HDGF agents in combination with chemotherapeutic agents and other anti-angiogenesis agents.

We have previously shown that HDGF may regulate expression of a panel of genes related to cancer cell invasion and extracellular matrix (ECM) formation, such as SERPIN2 and AXL (15). One of the mechanisms for HDGF induced mitogenesis is its binding to a yet identified surface receptor (16). It is possible that HDGF, secreted or released from tumor cells, bind to the surface receptor or enter into both tumor cells and adjacent stroma cells to function in autocrine and paracrine manner. Cytotoxic agents, such as Gem, may trigger an increased HDGF release from tumor cells. The antibody may neutralize extracellular HDGF and therefore shows a synergistic effect when combined with cytotoxic agents. The effect of our strategy to tumor microenvironment is particularly significant in anti-cancer therapy and warrants further investigation. When the anti-HDGF antibody was used together with Gem and bevacizumab, we observed an enhanced anti-tumor activity. This is probably due to HDGF and VEGF might play different roles in tumor angiogenesis. Therefore, simultaneous neutralizing both growth factors might have blocked multiple mechanisms contributing to angiogenesis and resulted in the enhanced anti-tumor activity. We are in the process to further investigate potential mechanisms involved in the anti-tumor activity.

Supplementary Material

Refer to Web version on PubMed Central for supplementary material.

Acknowledgments

This work was supported by Department of Defense grant DAMD17-01-1-01689-1 and National Cancer Institute grant CA126818.

References

1. Jemal A, Murray T, Samuels A, Ghafoor A, Ward E, Thun MJ. Cancer Statistics, 2006. CA Cancer J Clin 2006;56:106–30. [PubMed: 16514137]
2. Mountain CF. Revisions in the international system for staging lung cancer. Chest 1997;111:1700–23.
3. Crino L, Cappuzzo F. Present and Future Treatment of Advanced Non–Small Cell Lung Cancer. Semin Oncol 2002;29:9–16. [PubMed: 12094333]
4. Klastersky J, Paesmans M. Response to chemotherapy, quality of life benefits and survival in advanced non-small cell lung cancer: review of literature results. Lung Cancer 2001;34:S95–101. [PubMed: 11742711]
5. Everett AD, Stoops T, McNamara CA. Nuclear targeting is required for hepatoma-derived growth factor-stimulated mitogenesis in vascular smooth muscle cells. J Biol Chem 2001;276:37564–8. [PubMed: 11481329]
6. Nakamura H, Kambe H, Egawa T, et al. Partial purification and characterization of human hepatoma-derived growth factor. Clin Chim Acta 1989;183:273–84. [PubMed: 2553304]
7. Nakamura H, Izumoto Y, Kambe H, et al. Molecular cloning of complementary DNA for a novel human hepatoma-derived growth factor. Its homology with high mobility group-1 protein. J Biol Chem 1994;269:25143–9. [PubMed: 7929202]

8. Everett AD. Identification, cloning, and developmental expression of hepatoma-derived growth factor in the developing rat heart. Dev Dyn 2001;222:450–8. [PubMed: 11747079]
9. Lepourcelet M, Tou L, Cai L, et al. Insights into developmental mechanisms and cancers in the mammalian intestine derived from serial analysis of gene expression and study of the hepatoma-derived growth factor (HDGF). Development 2005;132:415–27. [PubMed: 15604097]
10. Ren H, Tang X, Lee JJ, et al. Expression of hepatoma-derived growth factor is a strong prognostic predictor for patients with early-stage non-small cell lung cancer. J Clin Oncol 2004;22:3230–7. [PubMed: 15310766]
11. Iwasaki T, Nakagawa K, Nakamura H, Takada Y, Matsui K, Kawahara K. Hepatoma-derived growth factor as a prognostic marker in completely resected non-small-cell lung cancer. Oncol Rep 2005;13:1075–80. [PubMed: 15870924]
12. Hu TH, Huang CC, Liu LF, et al. Expression of hepatoma-derived growth factor in hepatocellular carcinoma. Cancer 2003;98:1444–56. [PubMed: 14508832]
13. Yamamoto S, Tomita Y, Hoshida Y, et al. Expression of hepatoma-derived growth factor is correlated with lymph node metastasis and prognosis of gastric carcinoma. Clin Cancer Res 2006;12:117–22. [PubMed: 16397032]
14. Uyama H, Tomita Y, Nakamura H, et al. Hepatoma-derived growth factor is a novel prognostic factor for patients with pancreatic cancer. Clin Cancer Res 2006;12:6043–8. [PubMed: 17062679]
15. Zhang J, Ren H, Yuan P, Lang W, Zhang L, Mao L. Down-regulation of hepatoma-derived growth factor inhibits anchorage-independent growth and invasion of non-small cell lung cancer cells. Cancer Res 2006;66:18–23. [PubMed: 16397209]
16. Abouzied MM, El-Tahir HM, Prenner L, Häberlein H, Gieselmann V, Frnken S. Hepatoma-derived growth factor. Significance of amino acid residues 81–100 in cell surface interaction and proliferative activity. J Biol Chem 2005;280:10945–10954. [PubMed: 15655245]
17. Okuda Y, Nakamura H, Yoshida K, et al. Hepatoma-derived growth factor induces tumorigenesis in vivo through both direct angiogenic activity and induction of vascular endothelial growth factor. Cancer Sci 2003;94:1034–41. [PubMed: 14662017]
18. Everett AD, Narron JV, Stoops T, Nakamura H, Tucker A. Hepatoma-derived growth factor is a pulmonary endothelial cell-expressed angiogenic factor. Am J Physiol Lung Cell Mol Physiol 2004;286:L1194–201. [PubMed: 14751852]
19. Sandler A, Gray R, Perry MC, et al. Paclitaxel-carboplatin alone or with bevacizumab for non-small-cell lung cancer. N Engl J Med 2006;355:2542–50. [PubMed: 17167137]
20. Herbst RS, O'Neill VJ, Fehrenbacher L, et al. Phase II study of efficacy and safety of bevacizumab in combination with chemotherapy or erlotinib compared with chemotherapy alone for treatment of recurrent or refractory non-small-cell lung cancer. J Clin Oncol 2007;25:4743–50. [PubMed: 17909199]

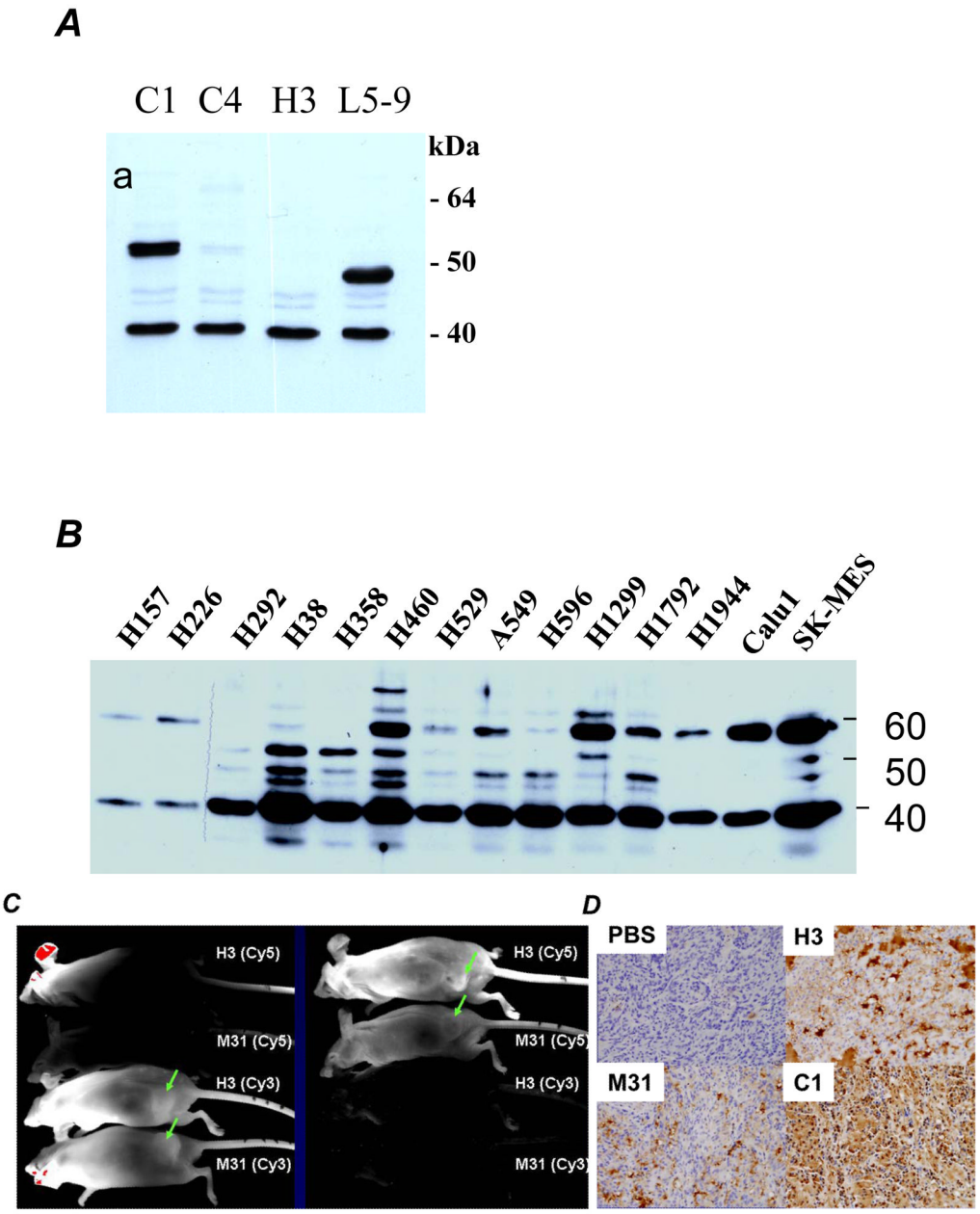

Figure 1.

A, Western blot analysis testing various monoclonal antibodies developed to against HDGF (lysate derived from H1944 cells). ***B***, HDGF in medium conditioned with various NSCLC cell lines (detected by using pooled monoclonal antibodies). ***C***, distribution of the antibodies in mice 12 hrs after IP injection. The antibodies and fluorescent dyes used are labeled next to each mouse. The left panel was an image captured using a filter for Cy3 dye whereas the right panel was an image captured using a filter for Cy5 dye. The arrows indicate locations of tumors. ***D***, distribution of the antibodies in tumor tissue sections (detected by using specific anti-mouse IgG). Antibodies used were labeled on the side of each section for easy reference.

A

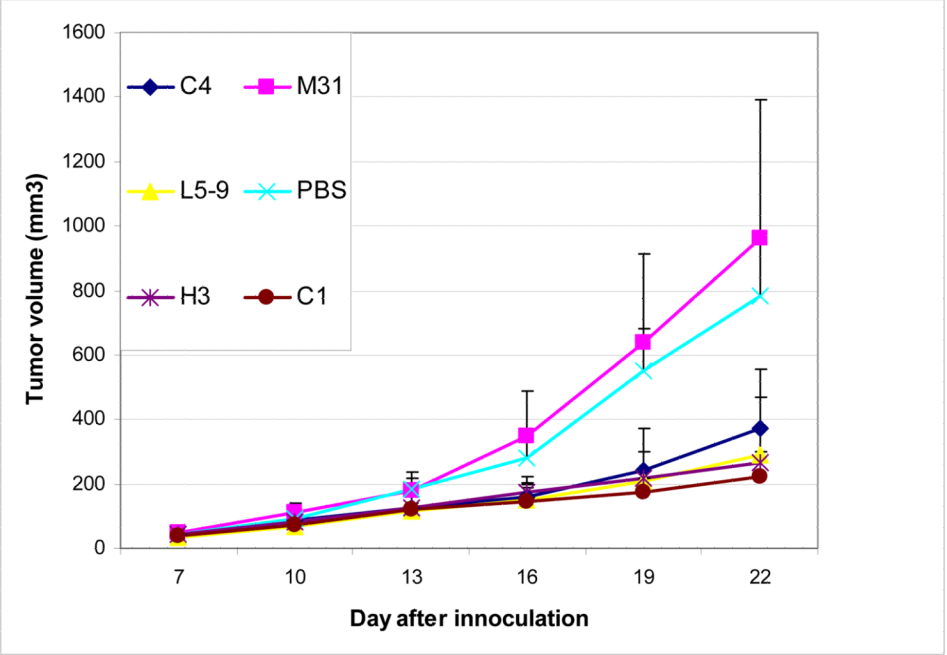

B

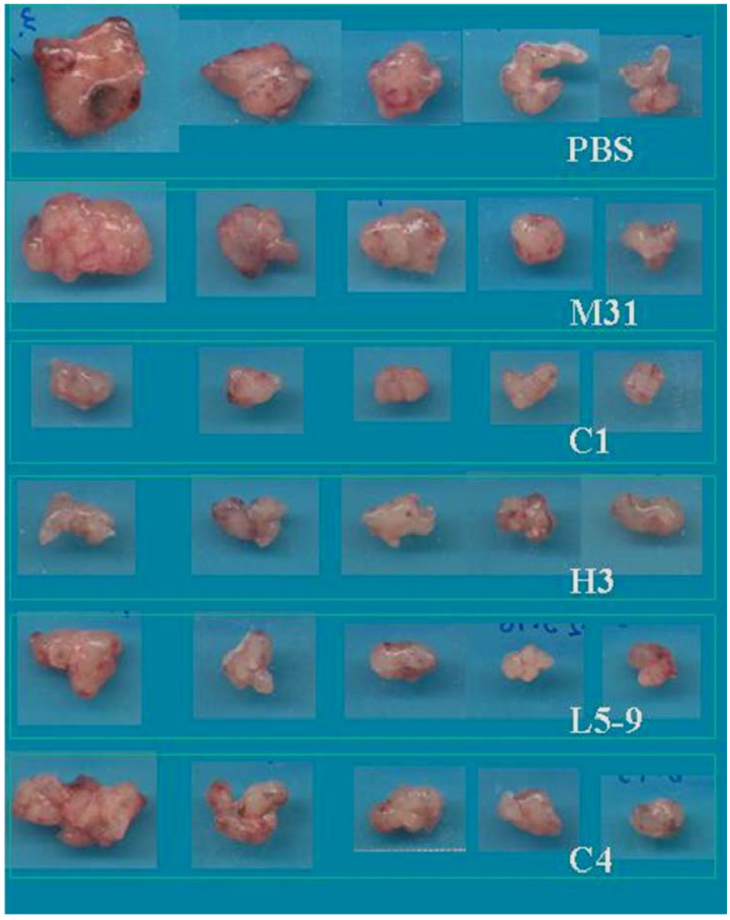

C

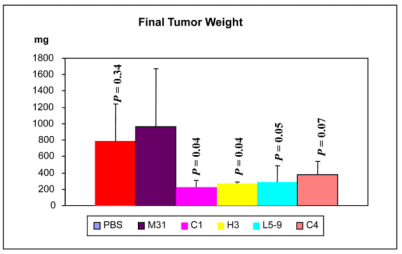

D

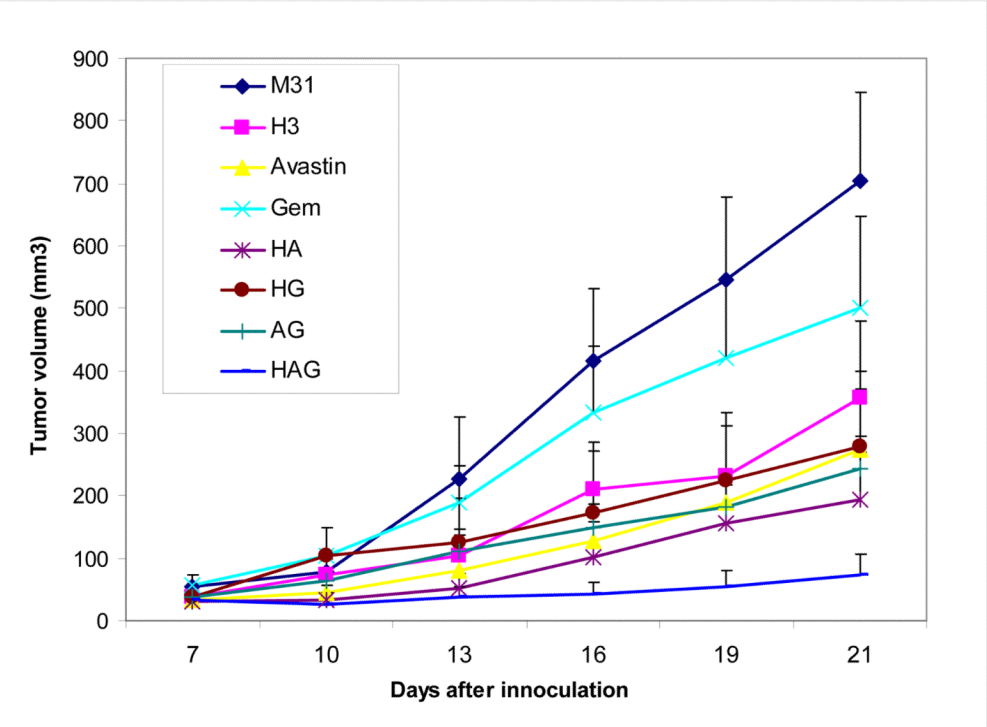

Figure 2.

A549 xenograft model. ***A***, growth curves of tumors treated with various antibodies. ***B***, tumors resected at the end of the experiment. ***C***, tumor weight measured for each treatment groups. *P* values are based on comparisons to M31 control group. ***D***, growth curves of tumors treated with single and combination of agents indicated in the right box. G, gemcitabine; A, bevacizumab; H, anti-HDGF-H3.

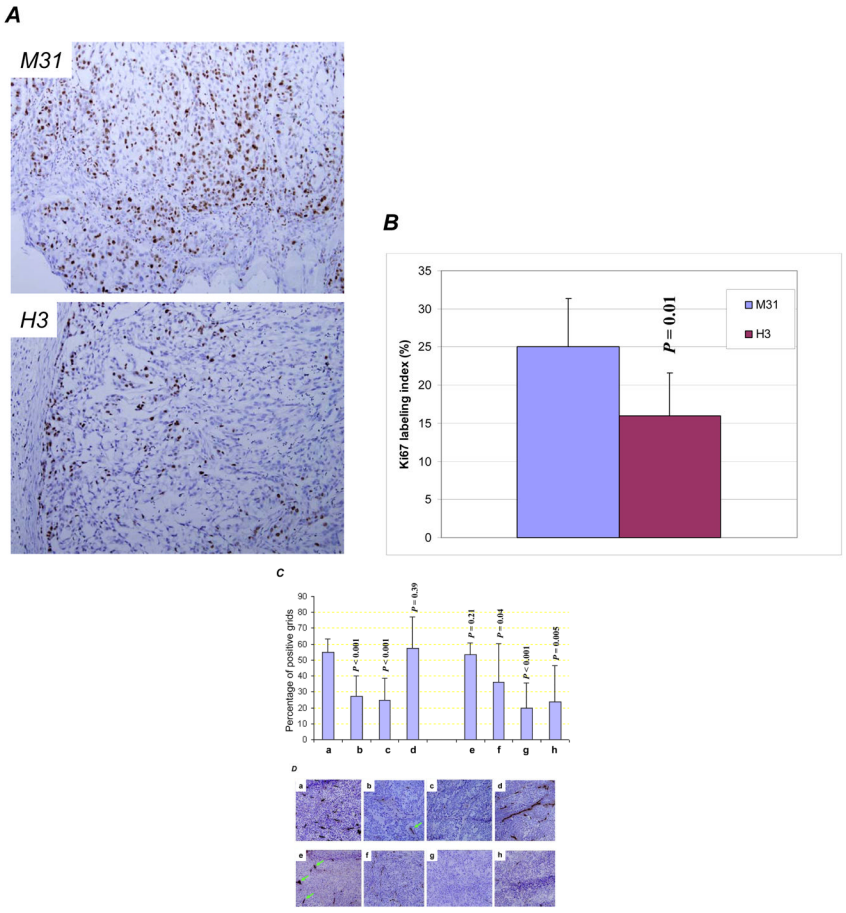

Figure 3.

Ki-67 expression in M31 and H3 treated tumors (**A**) and respective Ki-67 labeling indices in the two groups of tumors (**B**). Microvessel density measured by CD31 staining (**C**) with examples (**D**). ***a***, M31 antibody treatment; ***b***, bevacizumab treatment; ***c***, H3 antibody treatment; ***d***, Gemcitabine treatment; ***e***, bevacizumab combined with Gemcitabine; ***f***, H3 antibody combined with Gemcitabine; ***g***, H3 antibody combined with bevacizumab; ***h***, H3 antibody combined with bevacizumab and Gemcitabine. *P* values are based on comparisons to M31 control group and the error bars showing as standard deviations. Green arrows indicate microvessels with similar sizes as the controls.

A

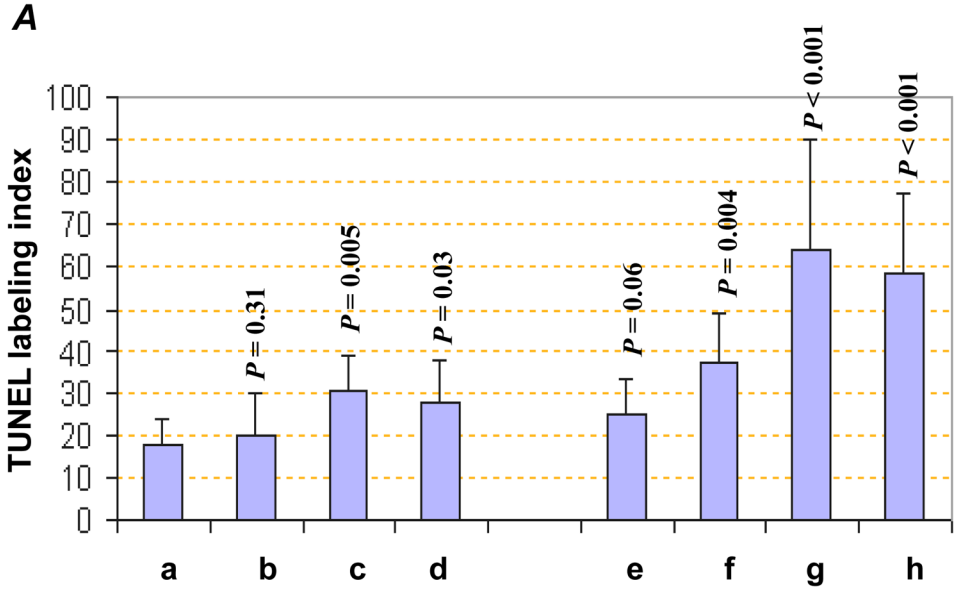

Comparison	c vs. g	d vs. f	g vs. h	f vs. h	e vs. h
P value	0.004	0.14	0.34	0.025	0.002

B

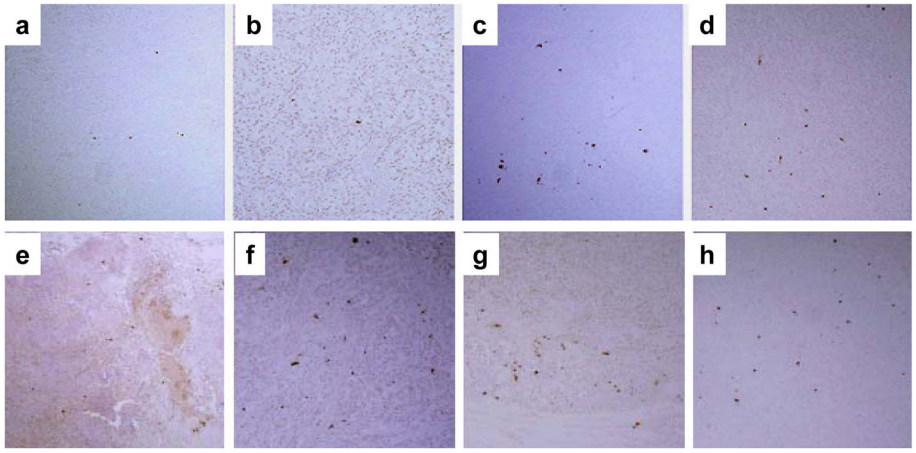

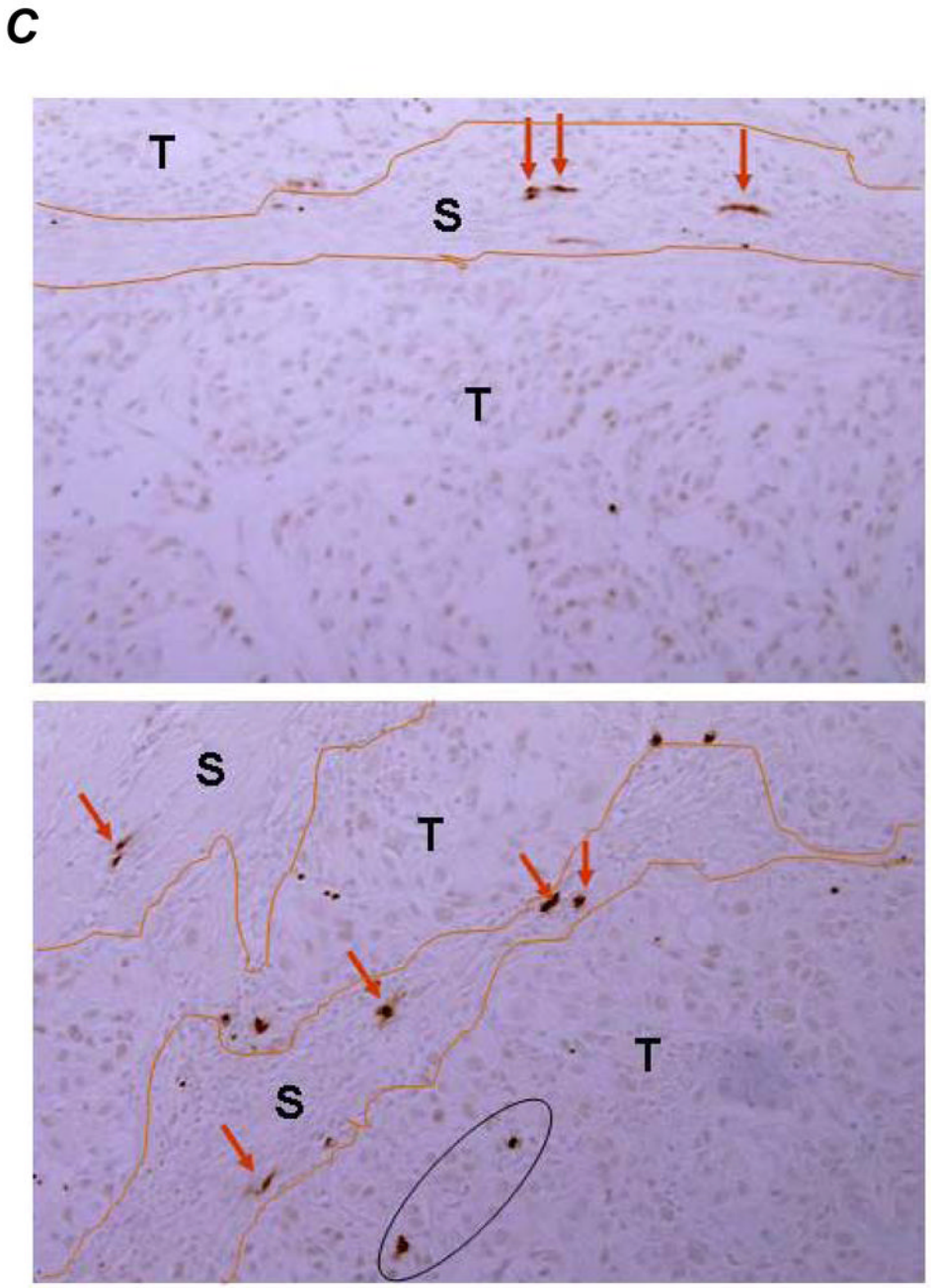

Figure 4.

TUNEL assay. **A**, TUNEL indices. *P* values are based on comparisons to M31 control group (upper panel) and comparisons listed in the table (lower panel). The error bars represent standard deviations. **B**, examples: ***a***, M31 antibody treatment; ***b***, bevacizumab treatment; ***c***, H3 antibody treatment; ***d***, Gemcitabine treatment; ***e***, bevacizumab combined with Gemcitabine; ***f***, H3 antibody combined with Gemcitabine; ***g***, H3 antibody combined with bevacizumab; ***h***, H3 antibody combined with bevacizumab and Gemcitabine. **C**, examples of apoptotic cells in tumor stroma were indicated by red arrows whereas the apoptotic tumor cells were inside a black cycle.